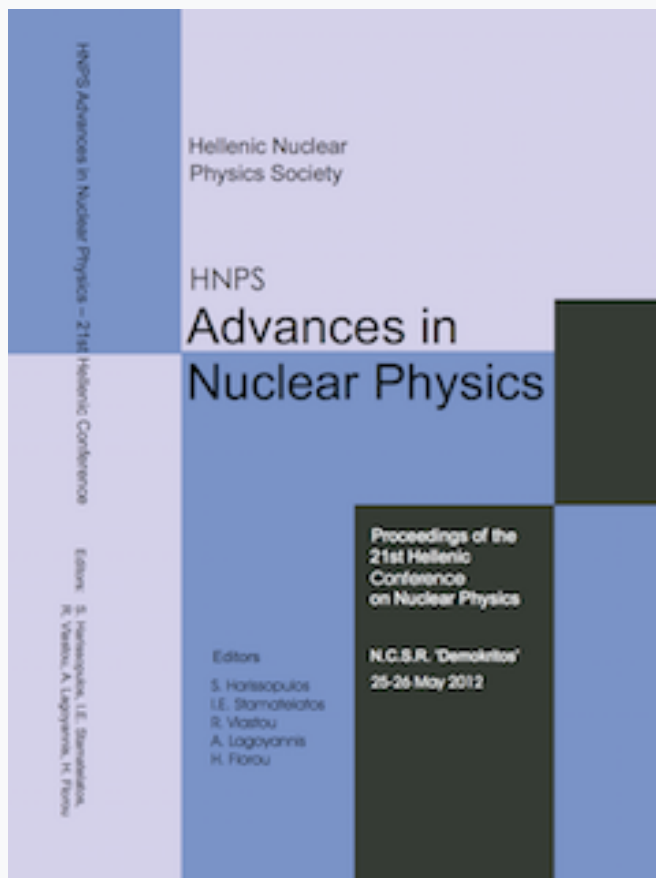


## HNPS Advances in Nuclear Physics

Vol 20 (2012)

HNPS2012



### Coherent neutrino scattering off the $^{48}\text{Ti}$ nucleus

*D. K. Papoulias, T. S. Kosmas*

doi: [10.12681/hnps.2494](https://doi.org/10.12681/hnps.2494)

#### To cite this article:

Papoulias, D. K., & Kosmas, T. S. (2012). Coherent neutrino scattering off the  $^{48}\text{Ti}$  nucleus. *HNPS Advances in Nuclear Physics*, 20, 104–111. <https://doi.org/10.12681/hnps.2494>

# Coherent neutrino scattering off the $^{48}\text{Ti}$ nucleus

D.K. Papoulias and T.S. Kosmas

*Division of Theoretical Physics, University of Ioannina, GR 45110 Ioannina, Greece*

---

## Abstract

The method of fractional occupation probabilities of the orbits is adopted in order to obtain nuclear form factors to be used for reliable cross sections calculations of the dominant coherent neutrino-nucleus reaction channel. To this purpose, the multipole decomposition method of Donnelly-Walecka is employed. The response of the  $^{48}\text{Ti}$  nucleus in solar and Supernova neutrino detection is investigated through our realistic nuclear structure cross sections calculations, based on the solution of the BCS equations. The present results indicate that the momentum dependence of the nuclear form factors cannot be neglected from the cross section, especially in the energy region of Supernova neutrinos (or for neutrinos having higher energies), because differences of even orders of magnitude may occur.

---

## 1 Introduction

Coherent neutrino-nucleus scattering, which is the dominant reaction channel, is widely recognised as an excellent probe for exploring astrophysical phenomena [1–3], for deeper understanding the Supernova (SN) explosion mechanisms, as well as for investigating the interior of distant stars [4,5]. Moreover, the exotic neutrino-nucleus reactions, offer interesting probes to investigate new physics beyond the Standard Model (SM). Such possible, lepton flavour violating (LFV) processes have the form  $\nu_\alpha(\tilde{\nu}_\alpha) + (A, Z) \rightarrow \nu_\beta(\tilde{\nu}_\beta) + (A, Z)$ , where  $\alpha \neq \beta$  [6]. The LFV parameters entering the latter flavour changing neutral current (FCNC) reactions, can be constrained from recent and future very sensitive experiments searching for exotic  $\mu^- \rightarrow e^-$  conversion, like the COMET at J-PARC, JAPAN and the Project X at Fermilab, USA, using  $^{48}\text{Ti}$  and  $^{27}\text{Al}$  respectively, as nuclear targets [7,8].

In the present work, we make an attempt to investigate in detail the response of the  $^{48}\text{Ti}$  nucleus, due to its great experimental interest, according to the SM neutrino reactions represented by  $\nu_\alpha(\tilde{\nu}_\alpha) + (A, Z) \rightarrow \nu_\alpha(\tilde{\nu}_\alpha) + (A, Z)$ . We adopt the Donnelly-Walecka method [9–11] and solve the BCS equations [12],

to perform realistic and accurate cross sections calculations [13–15]. We also employ the method of fractional occupation probabilities of the states [16], based on analytic expressions, for evaluating the proton charge density distribution and the nuclear form factors [17,18], entering the coherent rate. To this purpose, we extend the previous studies, by introducing more parameters, with which we increase the number of "active" nucleons in a nuclear system. Then we compare the predictions with the experimental data [19].

## 2 Brief description of the formalism

### 2.1 Neutral current neutrino-nucleus cross sections

At low and intermediate energies, considered in the present study, any semileptonic process is described by an effective interaction Hamiltonian, written in terms of the leptonic  $j_\mu^{\text{lept}}$  and hadronic  $\mathcal{J}_\mu$  currents as

$$\mathcal{H}_{\text{eff}} = -\frac{G_F}{\sqrt{2}} j_\mu^{\text{lept}}(x) \mathcal{J}^\mu(x), \quad (1)$$

where  $G_F$  is the well-known Fermi constant. In the Donnelly-Walecka multipole decomposition method, the neutral current double differential SM cross section from an initial  $|J_i\rangle$  to a final  $|J_f\rangle$  nuclear state reads [1,10]

$$\frac{d^2\sigma_{i\rightarrow f}}{d\Omega d\omega} = \frac{G_F^2}{\pi} \frac{\epsilon_i \epsilon_f}{(2J_i + 1)} \left( \sum_{J=0}^{\infty} \sigma_{\text{CL}}^J + \sum_{J=1}^{\infty} \sigma_{\text{T}}^J \right), \quad (2)$$

where  $\epsilon_i$  ( $\epsilon_f$ ) is the initial (final) neutrino energy. The cross sections  $\sigma_{\text{CL}}^J$  (for the Coulomb-longitudinal operators) and  $\sigma_{\text{T}}^J$  (for the tensor operators) are defined in [10] and are written in terms of the matrix elements (ME) of seven basic irreducible tensor operators, which in our convention are [9,11]

$$\langle j_1 || T_i^J || j_2 \rangle = e^{-y} y^{\beta/2} \sum_{\mu=0}^{n_{\text{max}}} \mathcal{P}_\mu^{i,J} y^\mu, \quad i = 1, \dots, 7. \quad (3)$$

Therefore, their evaluation is necessary for performing nuclear cross sections calculations. The coefficients  $\mathcal{P}_\mu^{i,J}$ , have been computed recently in Refs.[9,11]. For coherent neutrino scattering, we are interested in the present paper, only the Coulomb operator,  $T_1^0 \equiv \mathcal{M}_{00}$  (see, Eq.(8)), contributes. Then, the differential cross section with respect to the scattering neutrino angle becomes [14]

$$\frac{d\sigma}{d\cos\theta} = \frac{G_F^2}{8\pi} E_\nu^2 (1 + \cos\theta) Q_W^2 F^2(q^2), \quad (4)$$

where the weak charge is defined as  $Q_W = [(1 - 4 \sin^2 \theta_W) Z - N]$ . The kinematics of the reaction, imply that the magnitude of the three momentum transfer, written in terms of the incoming neutrino energy  $E_\nu$  (for coherent scattering  $\epsilon_i = \epsilon_f \equiv E_\nu$ ) and the scattering angle  $\theta$  (laboratory frame), is

$$q^2 = 4E_\nu^2 \sin^2 \frac{\theta}{2}. \quad (5)$$

However, from an experimental physics point of view, experiments are more sensitive to the kinetic energy of the recoiling nucleus given by  $T = q^2/2M$ , rather than the orientation of the scattering neutrino. Thus, expressing the differential cross section with respect to the nuclear recoil energy  $T$ , in the low energy approximation  $T \ll E_\nu$ , one finds [15]

$$\frac{d\sigma}{dT} = \frac{G_F^2 M}{4\pi} \left(1 - \frac{MT}{2E_\nu^2}\right) Q_W^2 F^2(q^2), \quad (6)$$

where  $M$  stands for the mass of the target nucleus. It can be seen from Eqs.(4,6) that the nuclear form factor has been taken into account, which from a nuclear physics point of view cannot be neglected, due to the finite nuclear size.

More precise cross sections calculations become possible by explicitly solving the BCS equations [12]. The differential cross section reads

$$\frac{d\sigma}{d\cos\theta} = \frac{G_F^2}{2\pi} E_\nu^2 (1 + \cos\theta) |\langle g.s. || \hat{\mathcal{M}}_{00}(q) || g.s. \rangle|^2, \quad (7)$$

where the  $g.s. \rightarrow g.s.$  transition ME is given by

$$\langle g.s. || \hat{\mathcal{M}}_{00}(q) || g.s. \rangle = \frac{1}{2} [(1 - 4 \sin^2 \theta_W) Z F_Z - N F_N]. \quad (8)$$

In the latter equation the form factors for protons (neutrons) are

$$F_{N_n} = \frac{1}{N_n} \sum_j [j] \langle g.s. || j_0(qr) || g.s. \rangle (V_j^{p(n)})^2 \quad (9)$$

where  $[j] = \sqrt{2j+1}$ ,  $N_n = Z$  (or  $N$ ),  $V_j^{p(n)}$  are the BCS probability amplitudes, determined by solving iteratively the BCS equations and  $j \equiv (n\ell)j$  are the quantum numbers of the h.o. orbits included in the assumed model space. We note that, in the approximation of  $F_Z \approx F_N$  and  $|J_i^\pi\rangle = |g.s.\rangle \equiv |0^+\rangle$  for the ground state, Eq.(7) coincides with Eq.(4).

In the rest of this work, we describe an effective method towards obtaining the form factor which is compared with the simple shell-model predictions through nuclear cross sections calculations.

## 2.2 Evaluation of the form factors

The radial nuclear charge density distribution  $\rho(r)$ , for harmonic-oscillator (h.o.) wavefunctions, is written in the following form [17,18]

$$\rho(r) = \frac{1}{\pi^{3/2}b^3} e^{-(r/b)^2} \Pi\left(\frac{r}{b}, Z\right), \quad \Pi(\chi, Z) = \sum_{\lambda=0}^{N_{\max}} f_{\lambda} \chi^{2\lambda}, \quad (10)$$

where  $\chi = r/b$ , with  $b$  denoting the h.o. size parameter.  $N_{\max} = (2n + \ell)_{\max}$  stands for the number of quanta of the highest occupied proton (neutron) level and the coefficients  $f_{\lambda}$  are expressed as [16]

$$f_{\lambda} = \sum_{(n,\ell)j} \frac{\pi^{1/2}(2j+1)n! C_{n\ell}^{\lambda-\ell}}{2\Gamma\left(n + \ell + \frac{3}{2}\right)} \quad (11)$$

where  $\Gamma(x)$  is the Gamma function. The nuclear form factor, which is the Fourier transform of the nuclear charge distribution density, after a straightforward manipulation can be cast as

$$F(q^2) = \frac{1}{Z} \int \rho(r) j_0(qr) d^3r, \quad (12)$$

with  $j_0$  being the zero order spherical Bessel function. It has been shown that, by using the charge density distribution of Eq.(10), the form factor  $F(q^2)$ , reads [17,18]

$$F(q^2) = \frac{1}{Z} e^{-(qb)^2} \Phi(qb, Z), \quad \Phi(qb, Z) = \sum_{\lambda=0}^{N_{\max}} \theta_{\lambda} (qb)^{2\lambda}. \quad (13)$$

The expression giving the coefficients  $\theta_{\lambda}$  is given in Ref.[18]. For a detailed description and further information, the reader is referred to Refs.[16–18].

Up to now, it has been considered that the occupation probabilities,  $a_{n\ell j}$ , are equal to unity for the states below the Fermi surface and zero for those above it. In Ref.[16], the authors introduced depletion and occupation numbers,  $\alpha_i$ , as parameters to describe the partially occupied levels of the states. The following relation should be satisfied

$$\sum_{\substack{(n\ell)j \\ \text{all}}} a_{n\ell j} (2j+1) = N_n, \quad (14)$$

where  $N_n$  is the number of protons or neutrons respectively. Hence, in this approximation, the "active" surface nucleons, (above or below the Fermi level) have non-zero occupation probability  $a_{n\ell j} \neq 0$  (smaller than unity), while the "core" levels have occupation probability  $a_{n\ell j} = 1$ . Extending the work of Ref.[16], where three parameters  $\alpha_1, \alpha_2, \alpha_3$  were used to describe the occupation probabilities, we now use  $\alpha_i, i = 1, 2, 3, 4$  parameters (for the definition

of  $\alpha_i$ , see in Ref.[16]). Therefore, in this parametrization, five single-particle are assumed as "active", and Eq.(16) of Ref.[16] becomes

$$\begin{aligned}
 \Pi(\chi, Z, \alpha_i) = & \Pi(\chi, Z_2) \frac{\alpha_1}{Z_1 - Z_2} + \Pi(\chi, Z_1) \left[ \frac{\alpha_2}{Z_c - Z_1} - \frac{\alpha_1}{Z_1 - Z_2} \right] \\
 & + \Pi(\chi, Z_c) \left[ \frac{Z' - Z}{Z' - Z_c} - \frac{\alpha_2}{Z_c - Z_1} - \frac{\alpha_3}{Z' - Z_c} \right] \\
 & + \Pi(\chi, Z') \left[ \frac{Z - Z_c}{Z' - Z_c} + \frac{\alpha_3}{Z' - Z_c} - \frac{\alpha_4}{Z'' - Z'} \right] \\
 & + \Pi(\chi, Z'') \left[ \frac{\alpha_4}{Z'' - Z'} - \frac{\lambda}{Z''' - Z''} \right] + \Pi(\chi, Z''') \frac{\lambda}{Z''' - Z''},
 \end{aligned} \tag{15}$$

with  $\lambda = \alpha_1 + \alpha_2 - \alpha_3 - \alpha_4$ . By replacing the polynomial  $\Pi(\chi, Z)$  of Eq.(10) with the latter expression (and similarly for the form factor of Eq.(13)) and using the experimental data [19] for the  $^{48}\text{Ti}$  nucleus, we fit the parameters  $\alpha_i$ . In our analysis,  $Z_2 = 18$ ,  $Z_1 = 20$ ,  $Z = Z_c = 22$ ,  $Z' = 30$ ,  $Z'' = 34$ ,  $Z''' = 40$ .

### 3 Results and discussion

As a first step of our calculational procedure, we evaluated the  $\theta_\lambda$  and  $f_\lambda$  coefficients, required for the form factor and the proton charge density of the  $^{48}\text{Ti}$  nucleus. An inversion of the  $(n\ell)j$  levels, compared to that assumed in Ref.[16] results in the present work, in order to fit the experimental data for  $^{48}\text{Ti}$ . These coefficients are listed below. As mentioned in Ref.[16], an interchange of the sequence of the levels, does not affect the coefficients of the core orbits (e.g. our results for the  $^{40}\text{Ca}$  nucleus coincide with those of Ref.[16]). The resulting fractional occupation numbers that fit the charge density distribution with the experimental data [19] are,  $\alpha_1 = 1.0$ ,  $\alpha_2 = 1.5$ ,  $\alpha_3 = 0.35$ ,  $\alpha_4 = 0.1$ . The prediction of the method (which is in very good agreement with the experimental data) is compared with that of the simple shell-model, in Fig.1. We note that in the momentum transfer range of our interest (i.e.  $q < 2\text{fm}^{-1}$ ) the form factor has excellent behaviour. By inserting the form factors obtained as described above in Eqs.(13,15) the resulting cross sections calculations have a rather high confidence level. The next step of our study was to apply the form factor discussed previously and using Eqs.(4,6) to perform nuclear cross sections calculations (see Fig.2). We note that large differences appear if the form factor dependence is neglected and hence  $F = 1$  is not reliable. However, at low neutrino energies, i.e.  $E_\nu \leq 20\text{MeV}$  that are relevant for solar neutrinos, the agreement of these two approximations is rather good. On the contrary, for the case of Supernova neutrinos (or neutrinos from other sources with higher energies), a difference of some orders of magnitude may exist. The scattering angle, has found to play significant role in the angular dependence of the differential cross section  $d\sigma/d\cos\theta$ . Forward scattering, ( $\theta = 0$ ) leads

$Z$	$(n\ell)j$	$\lambda = 0$	$\lambda = 1$	$\lambda = 2$	$\lambda = 3$	$\lambda = 4$
2	$0s_{1/2}$	2 (2)				
6	$0p_{3/2}$	6 (2)	$-\frac{2}{3} \left(\frac{8}{3}\right)$			
8	$0p_{1/2}$	8 (2)	-1 (4)			
14	$0d_{5/2}$	14 (2)	-3 (4)	$\frac{1}{10} \left(\frac{8}{5}\right)$		
18	$0d_{3/2}$	18 (2)	$-\frac{13}{3} (4)$	$\frac{1}{6} \left(\frac{8}{3}\right)$		
20	$1s_{1/2}$	20 (5)	-5 (0)	$\frac{1}{4} (4)$		
22	$1p_{1/2}$	22 (5)	$-6 \left(\frac{10}{3}\right)$	$\frac{13}{3} \left(\frac{4}{3}\right)$	$-\frac{1}{120} \left(\frac{8}{15}\right)$	
30	$0f_{7/2}$	30 (5)	$-10 \left(\frac{10}{3}\right)$	$\frac{5}{6} \left(\frac{4}{3}\right)$	$-\frac{1}{56} \left(\frac{8}{7}\right)$	
34	$1p_{3/2}$	34 (5)	-12 (10)	$\frac{6}{5} (-4)$	$-\frac{29}{840} \left(\frac{232}{105}\right)$	
40	$0f_{5/2}$	40 (5)	-15 (10)	$\frac{3}{2} (-4)$	$-\frac{1}{24} \left(\frac{8}{3}\right)$	
50	$0h_{9/2}$	50 (5)	$-\frac{65}{3} (10)$	$\frac{5}{2} (-4)$	$-\frac{5}{56} \left(\frac{8}{3}\right)$	$\frac{1}{1512} \left(\frac{32}{189}\right)$

Table 1

The exact coefficients  $\theta_\lambda$  ( $f_\lambda$ ) which are required to determine the proton and neutron form factors (charge density distribution) up to  $^{50}\text{Sn}$ , within the chosen model space.

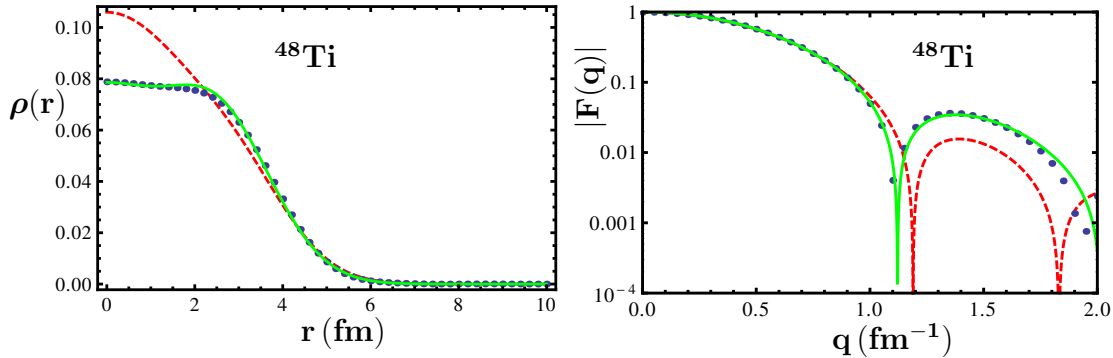


Fig. 1. The charge density distribution (*left*) and the form factor as a function of the momentum transfer (*right*), of the  $^{48}\text{Ti}$  nucleus. The experimental data are denoted with dots, the solid (green) line and the dashed (red) lines represent the predictions of the method of fractional occupation probabilities and single particle shell model respectively. We see that the introduction of fractional occupation probabilities of the states improves significantly the agreement with the experimental data.

to maximum  $d\sigma/d\cos\theta$  and obviously in that case the form factor is equal to unity due to zero momentum transfer, see Eq.(5).

A numerical integration of Eq.(4) yields the total coherent neutrino nucleus cross section and is compared to that for point-like nuclei where  $F = 1$ , see Fig.2. We observe that due to the different form factor dependence, the total cross section, in the range of incident neutrino energy  $E_\nu \gtrsim 80 \text{ MeV}$  and higher, appears to behave in a different way. The approximation  $F = 1$  gives

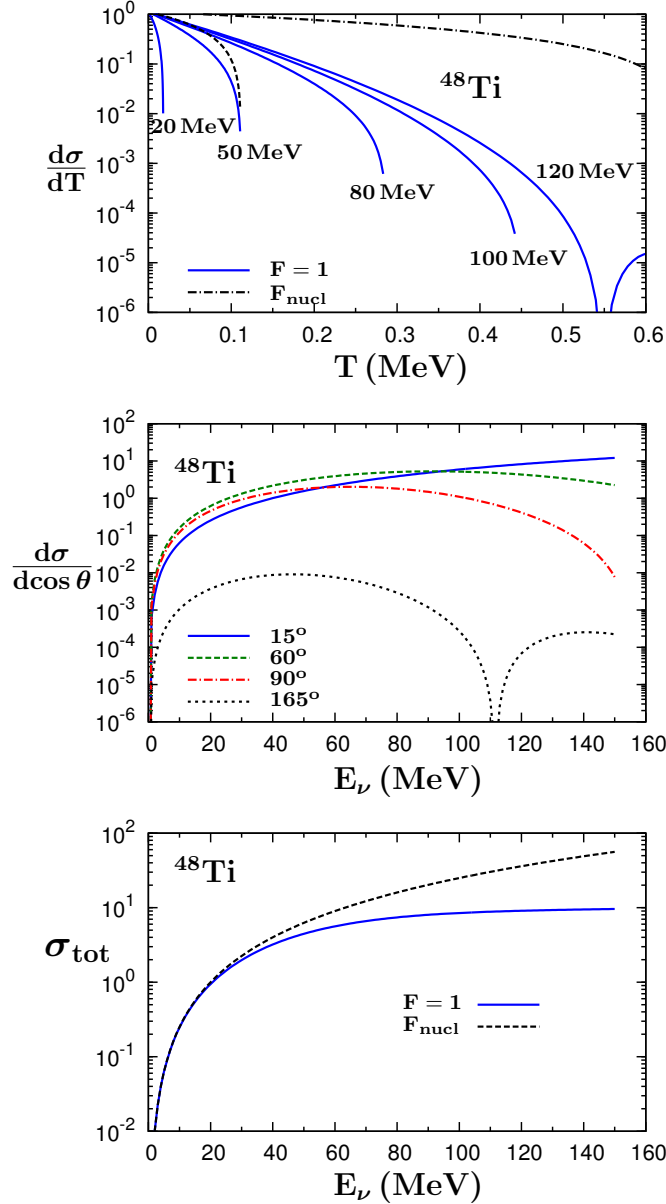


Fig. 2. *Top:* The differential cross section  $d\sigma/dT$  (in units  $10^{-37} \text{cm}^2/\text{MeV}$ ) as a function of the nuclear recoil energy  $T$  for various neutrino energies.  $d\sigma/dT$  is compared to that of point-like nucleus ( $F = 1$ ) for  $E_\nu = 50 \text{ MeV}$  and  $E_\nu = 120 \text{ MeV}$ . For rather low energies the results coincide, however for intermediate or high energies this is not the case.

*Middle:* The differential cross section  $d\sigma/d\cos\theta$  (in units  $10^{-39} \text{cm}^2$ ) as a function of the incoming neutrino energy  $E_\nu$ , for some typical angles. We observe the important affect of the scattering angle on  $d\sigma/d\cos\theta$ , e.g. for backward scattering, even not shown here, the cross section is minimized.

*Bottom:* The total coherent cross section,  $\sigma_{\text{tot}}$  (in units  $10^{-39} \text{cm}^2$ ) as a function of the incident neutrino energy in  $\text{MeV}$  (bottom), for  $^{48}\text{Ti}$ .  $\sigma_{\text{tot}}$  appears to have an asymptotic behaviour at neutrino energies  $E_\nu \gtrsim 80 \text{ MeV}$  or higher.

a rapidly increasing  $\sigma_{\text{tot}}$ , while our results indicate a slow increase. Moreover, the present results show that the ground state correlations which are necessarily included in the BCS, do not essentially affect the cross sections above  $E_\nu \gtrsim 80 \text{ MeV}$ .

## 4 Summary and Conclusions

In this work, we reported a general method for making realistic coherent neutrino-nucleus cross sections calculations in the context of the Donnelly-Walecka method, i.e. multipole expansion of the hadronic current. Comparing



with other methods (like the simple shell-model) and approximations (where the form factor is set equal to unity), we ended up with more reliable results. To this end, we obtained analytic expressions for the form factor (and also for the proton charge density), assuming fractional occupation probabilities with many parameters (fitted to the experimental data) and hence improving previous works. We concluded that, taking into account the momentum variation of the form factor is of significant importance, especially when we deal with Supernova neutrinos (or neutrinos with higher energies originating from other sources). We are currently working towards extending the present study, so as non-standard neutrino nucleus interactions will be included. We expect to come out with results in the context of theories going beyond the SM, using detailed nuclear structure calculations. Such results will be published elsewhere.

## References

- [1] T.W. Donnelly and R.D. Peccei, Phys. Rep. **50** (1979) 1.
- [2] P.S. Amanik, G. M. Fuller and B. Grinstein, Astropart. Phys. **24** (2005) 160.
- [3] P.S. Amanik and G.M. Fuller, Phys. Rev. **D 75** (2007) 083008.
- [4] V. Tsakstara and T.S. Kosmas, Phys. Rev. **C 83** (2011) 054612.
- [5] V. Tsakstara and T.S. Kosmas, Phys. Rev. **C 84** (2011) 064620.
- [6] J. Barranco et. al., JHEP **0512** (2005) 021.
- [7] Y.G. Cui et al. (COMET Collaboration), KEK Report 2009-10.
- [8] R. Bernstein and G. Kribs, talk at 2012 Project X Physics Study (PXPS12), Fermilab, June 14-28, 2012 Chicago USA.
- [9] D.K. Papoulias and T.S. Kosmas, J. Phys. Conf. Ser. **410** (2013) 012123.
- [10] T.W. Donnelly and J.D.Walecka, Nucl. Phys. **A 274** (1976) 368.
- [11] V.Ch. Chasioti and T.S. Kosmas, Nucl. Phys. **A 829** (2009) 234.
- [12] T.S. Kosmas et. al., Nucl. Phys. **A 570** (1994) 637.
- [13] D.Z. Freedman, et. al., Annu. Rev. Nucl. Sci. **27** (1977) 167.
- [14] A. Drukier and L. Stodolsky, Phys. Rev. **D 30** (1984) 2295.
- [15] J. Monroe and P. Fisher, Phys. Rev. **D 76** (2007) 033007.
- [16] T.S. Kosmas and J.D. Vergados, Nucl. Phys. **A 536** (1992) 72.
- [17] T.S. Kosmas and J.D. Vergados, Phys. Lett. **B 215** (1988) 460.
- [18] T.S. Kosmas and J.D. Vergados, Nucl. Phys. **A 510** (1990) 641.
- [19] H. De Vries et. al., At. Data and Nucl. Data Tables **36** (1987) 495536.